














# Adenylate kinase 9 is essential for sperm function and male fertility in mammals

Elena O'Callaghan<sup>a,1</sup>, Paula Navarrete-Lopez<sup>b,1</sup> , Miriama Štiavnická<sup>c</sup> , José M. Sánchez<sup>a,b</sup> , Maria Maroto<sup>b</sup>, Eva Pericuesta<sup>b</sup>, Raul Fernández-González<sup>b</sup> , Ciara O'Meara<sup>d</sup>, Bernard Eivers<sup>d</sup>, Margaret M. Kelleher<sup>e</sup>, Ross D. Evans<sup>e</sup>, Xena M. Mapel<sup>f</sup>, Audald Lloret-Villas<sup>f</sup> , Hubert Pausch<sup>f</sup> , Miriam Balastegui-Alarcón<sup>g</sup> , Manuel Avilés<sup>g</sup> , Ana Sanchez-Rodriguez<sup>h</sup>, Eduardo R. S. Roldan<sup>h</sup>, Michael McDonald<sup>a</sup> , David A. Kenny<sup>i</sup>, Sean Fair<sup>c</sup>, Alfonso Gutiérrez-Adán<sup>b,2,3</sup> , and Patrick Lonergan<sup>a,2,3</sup> 

Edited by Thomas Spencer, University of Missouri, Columbia, MO; received April 10, 2023; accepted August 23, 2023

Despite passing routine laboratory tests for semen quality, bulls used in artificial insemination exhibit significant variation in fertility. Routine analysis of fertility data identified a dairy bull with extreme subfertility (10% pregnancy rate). To characterize the subfertility phenotype, a range of *in vitro*, *in vivo*, and molecular assays were carried out. Sperm from the subfertile bull exhibited reduced motility and severely reduced caffeine-induced hyperactivation compared to controls. Ability to penetrate the zona pellucida, cleavage rate, cleavage kinetics, and blastocyst yield after IVF or AI were significantly lower than in control bulls. Whole-genome sequencing from semen and RNA sequencing of testis tissue revealed a critical mutation in adenylate kinase 9 (*AK9*) that impaired splicing, leading to a premature termination codon and a severely truncated protein. Mice deficient in *AK9* were generated to further investigate the function of the gene; knockout males were phenotypically indistinguishable from their wild-type littermates but produced immotile sperm that were incapable of normal fertilization. These sperm exhibited numerous abnormalities, including a low ATP concentration and reduced motility. RNA-seq analysis of their testis revealed differential gene expression of components of the axoneme and sperm flagellum as well as steroid metabolic processes. Sperm ultrastructural analysis showed a high percentage of sperm with abnormal flagella. Combined bovine and murine data indicate the essential metabolic role of *AK9* in sperm motility and/or hyperactivation, which in turn affects sperm binding and penetration of the zona pellucida. Thus, *AK9* has been found to be directly implicated in impaired male fertility in mammals.

sperm | bovine | mutation

Among all mammalian species, the confidence with which one can assign a fertility status to males is nowhere nearly as great as it is in bulls used in bovine artificial insemination (AI) due to the high number of inseminations and associated pregnancy and birth records per bull, sometimes reaching tens or even hundreds of thousands (1). The challenges in understanding the causes of poor fertility in monotocous species such as cattle (and humans) are quite different in males and females; in the female, reproductive success tends to be “all or nothing,” in that, typically, a single oocyte is ovulated and the female has, thus, one chance to become pregnant during each estrous cycle. In contrast, due to the high number of sperm deposited in the reproductive tract, an individual fertile sire has billions (natural mating) or millions (AI) of potential opportunities to get a female pregnant at each service event. In circumstances where a proportion of those gametes are compromised (e.g., after freeze-thawing), sufficient viable sperm can remain to effectuate a successful fertilization.

Fertility is among the most important economic traits in dairy production. Reproductive inefficiency at the farm level has a direct impact on overall herd profitability, particularly in seasonal calving dairy herds, by leading to longer calving intervals, reduced milk production, higher culling rates, and increased costs associated with intervention and labor (2). Due to the breeding structure of the industry, one subfertile bull can have a much greater impact on overall herd fertility than a single cow with fertility issues. Despite rigorous assessments of sperm quality before semen is released, significant variation in field fertility still exists among bulls used in AI (3). While bulls with sperm exhibiting severe morphological defects or significantly reduced sperm motility can be detected and removed, defects affecting capacitation, which confers on the sperm the ability to bind, to penetrate, and to fertilize the oocyte, can escape detection. For example, we previously reported an inherited recessive mutation in the transmembrane protein 95 (*TMEM95*) in bulls (4) associated with exceptionally poor reproductive performance due to failure of the sperm to penetrate the oocyte (5, 6), something which was subsequently validated in mice by us (6) and others (7).

## Significance

Fertility is among the most important economic traits in livestock production. Despite passing routine laboratory tests of semen quality, bulls used in artificial insemination exhibit a significant range in field fertility. Furthermore, the widespread use of individual sires potentially promotes the propagation of recessive conditions. We have identified a variant in the adenylate kinase 9 (*AK9*) gene that is correlated with severely impaired sperm function and extreme subfertility in bulls. Knockout mice deficient in *AK9* are completely infertile due to impaired sperm motility and an inability to penetrate the zona pellucida. Thus, *AK9* has been found to be directly implicated in impaired male fertility in mammals.

Author contributions: H.P., S.F., A.G.-A., and P.L. designed research; E.O., P.N.-L., M.Š., J.M.S., M. Maroto, E.P., R.F.-G., X.M.M., A.L.-V., H.P., M.B.-A., M.A., A.S.-R., E.R.S.R., M. McDonald, D.A.K., S.F., A.G.-A., and P.L. performed research; M.Š., C.O., B.E., M.M.K., R.D.E., H.P., S.F., and A.G.-A. analyzed data; H.P., D.A.K., S.F., and A.G.-A. obtained funding; P.L. obtained funding; and P.L. wrote the paper.

The authors declare no competing interest.

This article is a PNAS Direct Submission.

Copyright © 2023 the Author(s). Published by PNAS. This article is distributed under [Creative Commons Attribution-NonCommercial-NoDerivatives License 4.0 \(CC BY-NC-ND\)](https://creativecommons.org/licenses/by-nc-nd/4.0/).

<sup>1</sup>E.O. and P.N.-L. contributed equally to this work.

<sup>2</sup>A.G.-A. and P.L. contributed equally to this work.

<sup>3</sup>To whom correspondence may be addressed. Email: pat.lonergan@ucd.ie or agutierrez@inia.csic.es.

This article contains supporting information online at <https://www.pnas.org/lookup/suppl/doi:10.1073/pnas.2305712120/-/DCSupplemental>.

Published October 9, 2023.

Here, we present a detailed phenotypic and molecular characterization of an intronic variant in cattle that activates cryptic splicing of the adenylate kinase 9 (*AK9*) gene resulting in extreme subfertility associated with impaired sperm hyperactivation, failure of oocyte binding/penetration, and low frequency of embryo development culminating in severely compromised field fertility. To further investigate the role of AK9 in male fertility, we generated AK9-deficient knockout mice using CRISPR/Cas9 technology; *Ak9* knockout resulted in immotile sperm with a high incidence of abnormalities, reduced ATP levels, and impaired fertilization capacity. RNA-seq analysis demonstrated differential expression of genes involved in axoneme and sperm flagella components, as well as steroid metabolic processes. Ultrastructural analysis of sperm revealed a higher percentage of abnormalities in the flagella structure of mice.

## Results

**Field Fertility of FR4854.** Frozen-thawed semen from a Holstein Friesian AI sire (FR4854) was released into the Irish market in Spring 2020. Despite passing routine semen quality control checks, the bull had a phenotypic pregnancy rate of approximately 10% ( $n = 2,325$  inseminations), which was substantially lower than the mean ( $\pm$ SD) of  $57.0 \pm 0.05\%$  (range: 39.2 to 74.4%) for other Holstein Friesian sires used in the 2020 breeding season ( $n = 286$  bulls; range: 200 to 36,214 inseminations) (*SI Appendix, Fig. S1*). FR4854 has 371 recorded calves of which at least 17 are genotyped and sire verified to him (8 males, 9 females) confirming extreme subfertility but not total infertility. For parentage validation and prediction, ICBF uses 800 SNP (ICBF800) selected based on SNP clustering quality, ISAG200 inclusion, call rate, and minor allele frequency in the Irish cattle population with a threshold of 1% mismatches (around 10 SNPs) (8).

**Sperm Morphology.** The overall incidence of sperm with normal morphology was  $60.0 \pm 4.7\%$  and did not differ between FR4854 and the control. Scanning and transmission electron microscopy did not reveal any ultrastructural defects of the sperm head or flagellum in sperm from a control fertile bull and FR4854. The axonemes of the flagella exhibited the typical assembly of nine outer microtubule doublets surrounding a central pair (*SI Appendix, Fig. S2*).

**Computer-Assisted Sperm Analysis and Flow Cytometry.** Irrespective of whether sperm were incubated in TALP or methycellulose (medium with increased viscosity), total motility and progressive motility were reduced at all incubation time points in FR4854 but were comparable to some of the other bulls of proven fertility (*SI Appendix, Fig. S3*). Curvilinear velocity (VCL) was reduced for FR4854 when compared to all six control bulls ( $P < 0.05$ ), while straight line velocity (VSL), average path velocity (VAP), and amplitude of lateral head movement (ALH) were lower for FR4854 compared to five of the six control bulls ( $P < 0.05$ ). Notably, significantly impaired caffeine-induced hyperactivation was observed for FR4854 compared to the control (Fig. 1A and *Movies S1* and *S2*). Flow cytometry did not distinguish any differences in sperm viability, acrosome integrity, membrane fluidity, membrane potential, superoxide production, or DNA fragmentation between FR4854 and a control fertile bull (*SI Appendix, Table S1*).

**Mucus Penetration Assay.** Sperm from FR4854 exhibited comparable ability to penetrate follicular phase cervical mucus in vitro compared to sperm from a control fertile bull (*SI Appendix, Fig. S4*).

**In Vitro Fertilization.** Cleavage rate at 48 h post insemination (hpi) was significantly lower in FR4854 compared to the control

( $P < 0.01$ ) (Fig. 1B). The proportion of advanced embryos (>5-cell stage) at 48 hpi, an indicator of embryo developmental competence, was lower in FR4854 compared to the control ( $P < 0.01$ ); in addition, most cleaved embryos were at the two-cell stage and many had an abnormal morphology, including asymmetric blastomere size and clear areas within the cytoplasm (Fig. 1C). Blastocyst yield on Days 6, 7, and 8 pi was lower in FR4854 ( $P < 0.01$ ) compared to the control and was not affected by increasing the sperm concentration used in IVF from  $1 \times 10^6$  to  $4 \times 10^6$  sperm/mL (Fig. 1B). The proportion of presumptive zygotes exhibiting two pronuclei at 17 hpi was 79.5% in the control bull and zero in FR4854 (Fig. 1C).

Sperm from FR4854 exhibited a very reduced capacity ( $P < 0.05$ ) to penetrate empty zonae compared to a control bull in terms of the mean number of sperm per zona (2.25 vs. 0.12, respectively), the proportion of zonae with at least one penetrating sperm (60.7% vs. 9.21%, respectively), and the maximum number of sperm/zona (20 vs. 2, respectively) (Fig. 1D–F).

**In Vivo Fertilization.** Following insemination of superovulated heifers, FR4854 exhibited significantly fewer accessory sperm and reduced fertilization, based on embryo cleavage, compared to the control. Overall recovery rate (structures recovered/number of CLs) following insemination was 57.8% and was not different between bulls. Fertilization rate (based on cleaved oocytes) was 73.3% vs 4.6% for the control and FR4854, respectively (*SI Appendix, Table S2*;  $P < 0.001$ ). The majority of embryos recovered from the control were at the >5-cell stage (mean number of cells recovered from control was 7.85 vs 1.24 for FR4854) (*SI Appendix, Fig. S5*). Mean ( $\pm$ SE) number of accessory sperm was  $1.44 \pm 0.48$  (range: 0–54) for the control and zero for FR4854.

**Candidate Causal Variants.** The genome of FR4854 was sequenced to 25.76-fold coverage using 150 bp paired-end libraries. Reference-guided variant discovery and genotyping yielded a total of 4,616,420 and 2,588,663 variants in FR4854 that were heterozygous and homozygous for a non-reference allele, respectively. Following our previous research (4, 9–12), we hypothesized that the extreme subfertility of FR4854 was due to a recessively inherited allele that is deleterious to protein function. Autozygosity mapping identified 64 runs of homozygosity that were longer than 1 Mb encompassing a total of 171.2 Mb autosomal sequence of FR4854 (*SI Appendix, Fig. S6*). Of the 2,588,663 sequence variants that were homozygous in FR4854, we identified 112 (Ensembl) and 111 (Refseq) that were i) not seen in the homozygous state in fertile control bulls and ii) predicted to be highly or moderately deleterious to protein function, including 29 that were within runs of homozygosity. We further assumed that the mutation should be relatively rare in cattle and predominantly limited to the Holstein lineage. Four of the 29 candidate causal variants had minor allele frequency less than 2%, were observed in the homozygous state in less than 10 (out of 5,116) animals of the latest run (Run9) of the 1,000 bull genomes project consortium (13), and were primarily found in Holstein animals (*SI Appendix, Table S3*).

Three compatible missense variants were within a run of homozygosity at the distal end of BTA1 affecting either *COL6A6* or *COL6A5*. A contribution of collagen type 6 to impaired fertility has not been described to date (14). Based on these observations and the fact that both genes are lowly expressed in testis tissue of mature bulls (less than 2 transcripts per million, TPM), we did not consider the missense variants in *COL6A6* and *COL6A5* as compelling candidate causal variants for the impaired fertility of FR4854. The remaining compatible variant was a missense variant (Chr9:40620329A>G, ENSBTAP00000020294.1:p.Ile678Val)

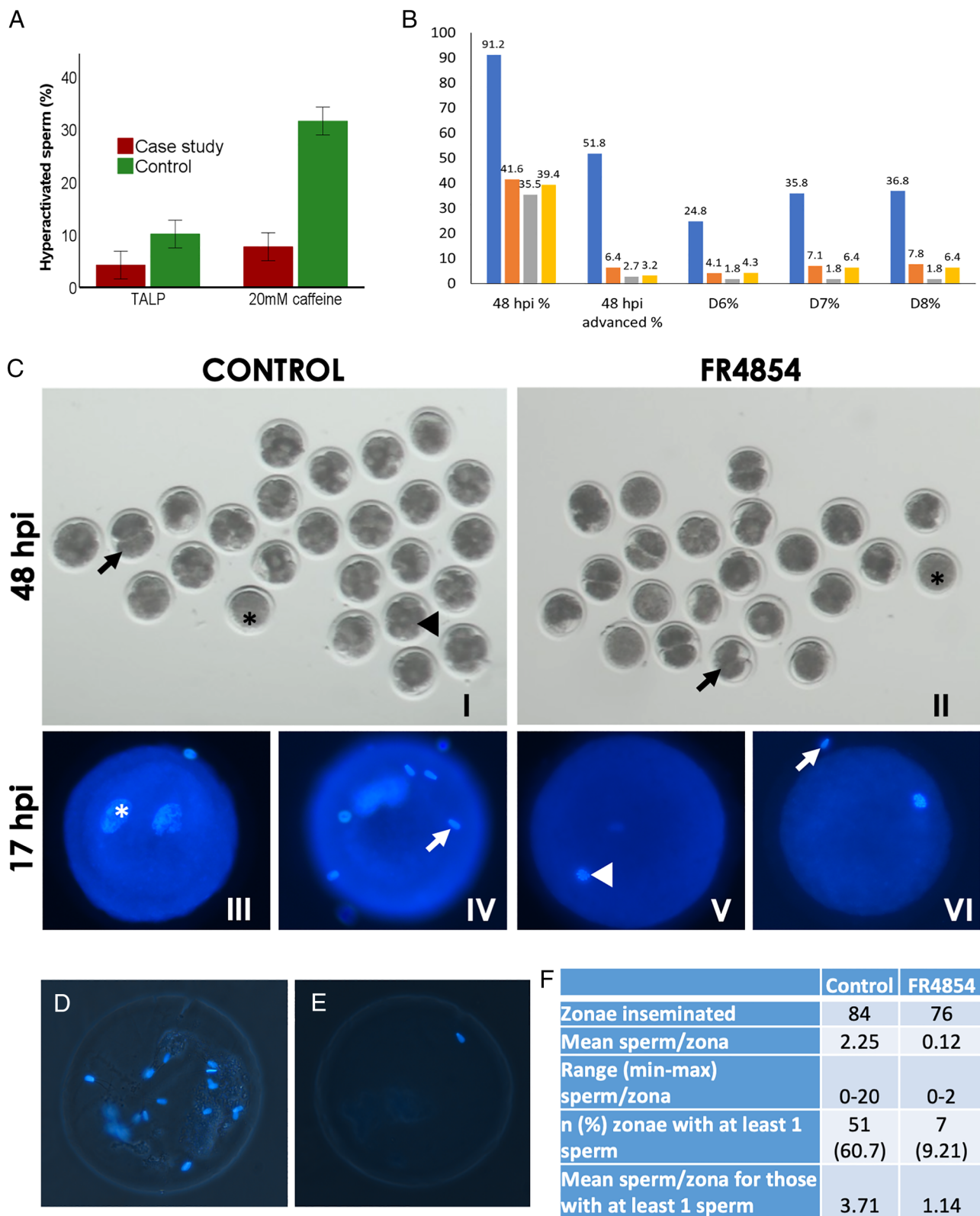


**Fig. 1.** (A) Sperm from FR4854 exhibited impaired ability to undergo hyperactivation ( $P < 0.05$ ) compared to the control. Hyperactivation was induced by 20 mM caffeine and immediately assessed by CASA. One straw from each of 3 ejaculates for each bull; mean  $\pm$  SE. (B) Cleavage and blastocyst development after in vitro fertilization of in vitro matured oocytes with semen from a control, highly fertile, bull (blue bars) or FR4854 at  $1 \times 10^6$  (orange bars),  $2 \times 10^6$  (gray bars) or  $4 \times 10^6$  (yellow bars) sperm/mL. Embryos cleaved by 48 h post insemination (hpi), advanced embryos (>5-cells) by 48 hpi, and blastocyst yield on days (D) 6, 7, and 8 were lower ( $P < 0.05$ ) in FR4854 compared to the control. Increasing sperm concentration did not have any effect. (C) Representative images of in vitro produced embryos at 48 hpi ( $C_I$ -control bull and  $C_{II}$ -FR4854) and presumptive zygotes at 17 hpi ( $C_{III}$  and  $C_{IV}$ -control bull and  $C_V$  and  $C_{VI}$ -FR4854). Note that most of the embryos in the control are at the 5- to 8-cell stage at 48 hpi, while all cleaved embryos for FR4854 except one are still at the 2-cell stage. Not cleaved (black asterisk); <5-cell embryos (black arrow); >5-cell embryos (black arrowhead). Metaphase II plate (white arrowhead); Pronucleus (white asterisk); Accessory sperm bound to the zona pellucida (white arrow). (D–F) Penetration of empty bovine zonae following oocyctectomy and insemination in vitro with sperm from a control fertile bull (D) or from FR4854 (E). Note the presence of multiple sperm in the control. (F) Table with the comparison of the penetration of empty zonae between control and FR4854.



in *AK9* encoding adenylate kinase 9. The Chr9:40620329 G-allele resides within an approximately 23.625 Mb long segment (between 35.50 Mb and 59.125 Mb) of very low heterozygosity in FR4854 (Fig. 2A). *Adenylate kinase 9* exhibits a testis-biased expression in mammals (e.g., <https://gtexportal.org/home/>, <https://cattlegeneatlas.roslin.ed.ac.uk/>) (15). In testis transcriptomes from 76 mature bulls, *AK9* (ENSBTAG00000010116) was transcribed in high abundance ( $35.85 \pm 6.70$  TPM; Fig. 2C).

**A Splice Variant of *AK9* is Associated with Low Fertility.** The Chr9:40620329A>G variant is predicted to result in a nonsynonymous substitution (ENSBTAP00000020294.1:p.Ile678Val) in the 17th exon of *AK9* according to the Ensembl (version 104) annotation of the bovine genome. However, the Refseq (version

106) annotation indicated that Chr9:40620329A>G resides in an intron of all three annotated *AK9* transcript isoforms (XM\_024996966.1, XM\_024996965.1, XM\_005210829.3). Bovine *AK9* has between 1,906 and 1,910 amino acids according to Refseq which is similar to different isoforms of human *AK9* [i.e. adenylate kinase 9 isoform 1 (NP\_001138600.2) has 1,911 amino acids]. However, the Ensembl annotation suggests that bovine *AK9* (ENSBTAP00000020294.6) has only 679 amino acids. We suspected that differences in amino acid lengths and the conflicting functional consequences predicted for the Chr9:40620329A>G variant between the Ensembl and Refseq annotations suggest that either one or both annotations contain flaws. Testis RNA sequencing read alignments from mature bulls contained many reads that spanned exon–exon junctions that were only included

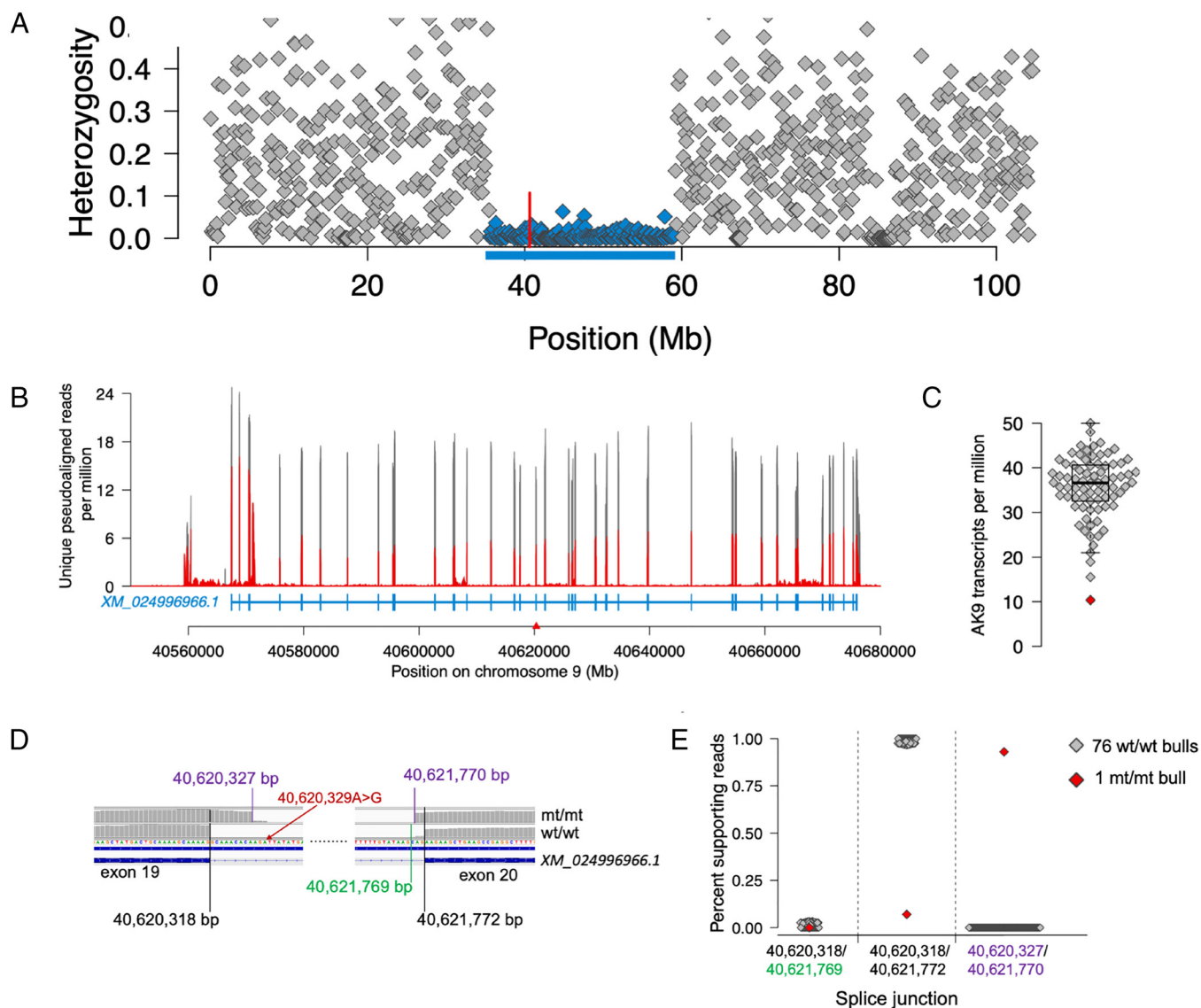


**Fig. 2.** (A) A candidate causal variant for the subfertility of the bull resides in a segment of extended autozygosity on BTA9. Each symbol represents the proportion of heterozygous genotypes observed in DNA sequencing data of FR4854 within 125 kb windows. Blue color represents all 125-Kb windows within a 23.625 Mb segment of extended homozygosity encompassing Chr9:40620329 (red vertical line). (B–D) The Chr9:40620329 G-allele activates cryptic splice donor and acceptor sites in *AK9* intron 19. (B) Average testis RNA sequencing coverage from 76 bulls homozygous for the Chr9:40620329 A-allele (gray color) and one bull homozygous for the Chr9:40620329 G-allele (red color) at the genomic region encompassing bovine *adenylate kinase 9* (XM\_024996966.1). The number of reads covering a genomic position was extracted from coordinate sorted STAR-aligned BAM files and subsequently divided by the total number of unique reads that were pseudoaligned during transcript abundance estimation with kallisto. Blue color indicates the exon–intron structure of bovine *AK9* as annotated in the Refseq database. The red triangle indicates the position of Chr9:40620329. (C) *AK9* transcript abundance [transcripts per million (TPM)] in testis tissue from 76 wt/wt (gray) and one mt/mt (red) bull (FR4854). (D) Annotated IGV screenshot of the RNA sequencing alignments for one mt/mt (FR4854) and one representative wt/wt bull at the splice donor and acceptor sites of *AK9* intron 19. Black color indicates the regular splice sites that are only rarely used in the mt/mt bull. Violet color indicates cryptic splice sites activated only in the mt/mt bull homozygous for the Chr9:40620329 G-allele. (E) Splice junction utilization in 76 bulls homozygous for the wild-type A-allele (gray color) and one bull homozygous for the mutant G-allele (red color).



in the Refseq annotation and had high coverage overlapping the respective coding sequences, thereby supporting that bovine *AK9* consists of 40 coding exons encoding 1,906 amino acids as indicated by the Refseq annotation (XP\_024852734.1) (Fig. 2 *B–E*). This confirms that the Ensembl annotation of bovine *AK9* (ENSBTAG00000010116) is both erroneous and incomplete.

The Chr9:40620329A>G variant is located in intron 19, 12 bases downstream of a non-canonical (GC) splice donor site, as correctly indicated by the Refseq annotation. Variant effect prediction based on the Refseq annotation suggests a “modifier” rather than a “nonsynonymous” consequence for Chr9:40620329A>G. However, the Chr9:40620329 G-allele introduces a novel GT dinucleotide which we hypothesized might serve as a cryptic yet canonical splice donor site. None of the animals of our eQTL mapping cohort carried the G-allele preventing immediate investigation of putative alternative splice site usage due to the Chr9:40620329A>G variant. To investigate the suspected impact of the Chr9:40620329 G-allele on *AK9* pre-mRNA splicing, we sequenced RNA extracted from testis tissue of FR4854 and mapped the reads against the reference genome using a splice-aware alignment software (16). Read coverage analysis showed that the Chr9:40620329 G-allele activates cryptic pre-mRNA splicing at both the splice donor and splice acceptor sites of intron 19. In FR4854, 93% of the RNA sequencing reads spanning the splice junction between exons 19 and 20 supported splice donor and acceptor sites at 40,620,327 bp and 40,621,770 bp, respectively (Fig. 2 *D* and *E*). These splice sites were not observed in 76 testis transcriptomes of mature bulls that were homozygous for the Chr9:40620329 A-allele. Among 8,754 cattle transcriptomes from the cattle GTEx atlas (17), these splice sites had low support (less than five junction-spanning reads) in 17 Holstein samples, and intermediate support (between 8 and 30 junction-spanning reads) in 8 Holstein samples confirming that they are rarely utilized. The remaining 7% of the splice junction-spanning reads observed in FR4854 supported the regular splice donor and acceptor sites at 40,620,318 bp and 40,621,772 bp that were the predominant ( $98.2 \pm 1.2\%$ ) splice sites in 76 bulls homozygous for the Chr9:40620329 A-allele.

Alternative splice site usage leads to a frameshift in translation from amino acid 724 onward. This frameshift eventually induces a premature translation codon at position 854 that leads to a truncated *AK9* protein that lacks 1,053 amino acids (55%) from the C-terminal region unless the transcript is subjected to nonsense-mediated mRNA decay. *AK9* mRNA was less abundant in FR4854 (10.36 TPM) than the 76 bulls ( $35.85 \pm 6.70$  TPM) homozygous for the wild-type allele at Chr9:40620329 (Fig. 2*C*). Differential expression between FR4854 and the wild-type bulls was evident for all *AK9* exons (Fig. 2*B*).

**Immunohistochemistry of Bovine Testes Tissue.** Representative images of cross-sections of seminiferous tubules stained with Hoechst, FITC-PNA, and anti-*AK9* are shown in *SI Appendix, Fig. S7*. No differences were observed between the structure of the seminiferous tubules of FR4854 and the control, containing a similar number of acrosome-positive cells. In the control testis, *AK9* was mainly located in the cytoplasm of spermatogonia and primary spermatocytes, but in Leydig cells, pachytene spermatocytes, and round spermatids, the protein signal was also nuclear (*SI Appendix, Figs. S6 D, VIII and S7 D, IX*). FR4854 did not express or expressed very little *AK9* protein mainly in the spermatogonial stage, but no expression was observed in spermatocytes or spermatids.

**Fertility of Half-Sibling Females of FR4854.** *SI Appendix, Fig. S8* illustrates the overall Economic Breeding Index (EBI), production subindex, fertility subindex, calving interval predicted transmitting ability (PTA), and survival PTA for female half-siblings of FR4854 compared to the 2020-born population. Interestingly, his half-siblings were behind the mean of the overall population for all traits except survival PTA.

**Phenotypes Associated with Murine *Ak9* Gene Disruption.** We generated *Ak9* knockout mice using CRISPR/Cas9 technology. Four lines were established by inducing deletions in exon 21 and between exon 21 and 23, resulting in altered protein forms with different lengths compared to the normal form (Fig. 3 *A–C*). The absence of the protein was confirmed through western blotting and immunohistochemistry (Fig. 3 *D* and *E*).

Both male and female edited mice developed normally. However, while females remained fertile, males with homozygous mutations were infertile. Despite normal appearances of seminiferous tubules and acrosomal caps in knockout mice (Fig. 4 *A* and *B*), the loss of *AK9* resulted in complete immotility of flagella (Fig. 4*G* and *Movies S3* and *S4*), which explains the observed sterility in male mice. Confirming this, intracytoplasmic sperm injection (ICSI) of sperm from *Ak9*<sup>-/-</sup> males with wild-type oocytes resulted in normal fertility and the birth of live offspring at rates similar to heterozygote or wild-type sperm (*SI Appendix, Table S4*). Reproductive parameters, including testis size, gonadosomatic index, and sperm concentration, were not different from those of wild-type mice (Fig. 4 *C, D*, and *F*). However, sperm from knockout males exhibited an increased frequency of morphological abnormalities, including defects in the head, midpiece, and flagellum (Fig. 4 *E* and *I* and  $P < 0.05$ ). Additionally, ATP levels in sperm collected in HTF medium containing glucose, pyruvate, and lactate were significantly lower in *Ak9*<sup>-/-</sup> sperm in comparison to their wild-type counterparts (Fig. 4*H*).

**Subcellular Localization of *AK9* in Mouse Testis.** Wild-type *AK9* was detected through immunohistochemistry in the seminiferous epithelium in pachytene spermatocytes and round spermatids and in the interstitial tissue in Leydig cells (*SI Appendix, Fig. S9*). In Leydig cells, *AK9* was strongly expressed in the cytoplasm, and also some cytoplasmic signal was observed in spermatogonia, preleptotene, leptotene spermatocytes, and round spermatids. Intense nuclear signal was observed in pachytene spermatocytes and in round spermatids (*SI Appendix, Fig. S9*).

**Differential Expression of Sperm Components.** RNA-seq analysis was performed on four testis samples from *Ak9* knockout mice (*Ak9*<sup>-/-</sup>) and four samples from wild-type mice. The analysis yielded an average of 25.2 million paired-end reads, with successful assignment of 18 to 24 million fragments against the reference annotation. Approximately 23,900 genes were detected (*Dataset S1*). One outlier sample with a distinct expression pattern was excluded from further analysis. The aligned reads revealed induced deletions in the *Ak9*<sup>-/-</sup> samples, specifically affecting exon 21, 22, and 23 (*SI Appendix, Fig. S10A*).

Using DEseq2, we identified a total of 1,093 differentially expressed genes (DEGs) with FDR < 0.05, including 745 up- and 339 down-regulated genes in *Ak9*<sup>-/-</sup> samples compared to wild-type samples (*Dataset S2*). A volcano plot and heatmap displayed the altered genes with FDR < 0.05 (*SI Appendix, Fig. S10 B and C*). There were 54 genes with a fold change > 2 at FDR < 0.05. As observed in the volcano plot (*SI Appendix, Fig. S10C*), one of the genes with the greatest difference in expression was carbonic anhydrase 3 (*Car3*), which was down-regulated with a log<sub>2</sub>(FC) of -6.07.

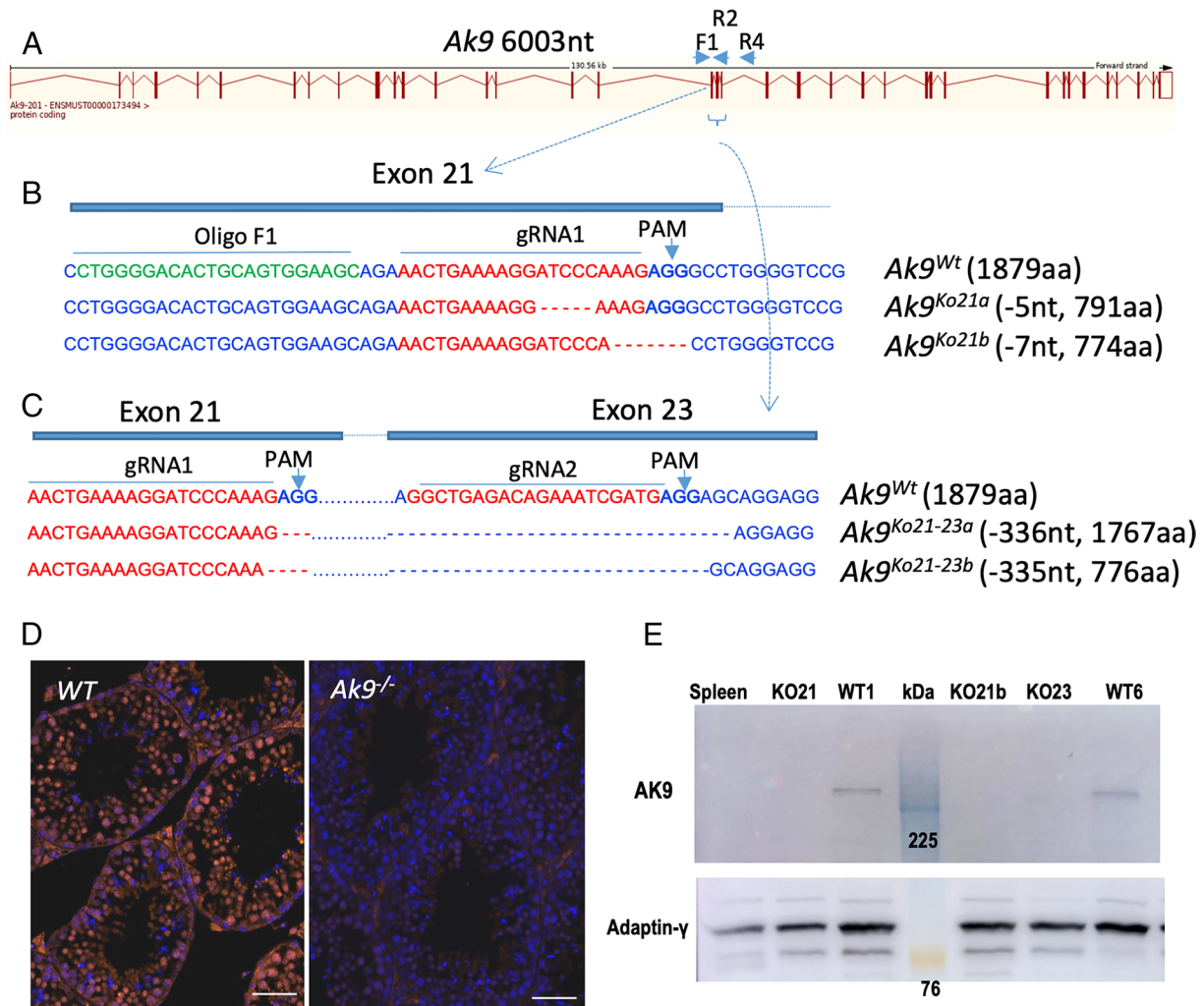


**Fig. 3.** Diagrams of *Ak9* gene structure, knockout lines produced by CRISPR/Cas9, and loss of AK9 protein expression. (A) Scheme of wild-type *Ak9* gene structure, composed of 41 exons. (B) Frameshift deletions of the different mutant lines produced by CRISPR/Cas9 in exon 21 (*Ak9*Ko21a and *Ak9*Ko21b) and (C) exon 21 and 23 (*Ak9*Ko21-23a and *Ak9*Ko21-23b). (D) Cross-sections of seminiferous tubules of WT and *Ak9*<sup>-/-</sup> stained with nuclear dye Hoeschst (blue) and anti-AK9 (orange). (E) Western blot of AK9 protein expression in the testes of 3 *Ak9*<sup>-/-</sup> and 2 WT, using  $\beta$ -3-adaptin as loading control.

To determine the cell stage in which the DEGs were expressed, we assigned the genes to specific cell types based on a single-cell RNA-seq dataset (18). Clustering identified four main cell types: spermatogonia, spermatocytes, spermatids, and somatic cells (SI Appendix, Fig. S10D). Integration of this analysis with our data revealed the assignment of DEGs to specific cell types: 776 genes in spermatocytes, 764 genes in spermatids, 415 genes in spermatogonia, 401 genes in Sertoli cells, 171 genes in other somatic cells, 143 genes in Leydig cells, 94 genes in sperm, and 47 genes unclassified (Dataset S3). These findings suggest that the knockout of *Ak9* had varying impacts on the transcriptome of different testis cell types. Notably, the majority of up-regulated genes were expressed in spermatids (SI Appendix, Fig. S10 D and E).

Overrepresentation analysis detected the GO biological processes (GO-BP), cellular components and molecular functions (GO-MF), as well as KEGG pathways significantly enriched (FDR < 0.05) in the set of DEGs (Dataset S4). Interestingly, up-regulated genes were associated with cilium- and flagellum-dependent motility, axoneme and flagellum assembly, microtubule movement, spermatid differentiation, sperm-egg recognition, and fertilization (Fig. 5A). Accordingly, the subcellular structures where a significant proportion of up-regulated gene products are located include different parts of the sperm structure, such as flagellum, axoneme, sperm

principal piece, midpiece, connecting piece, fibrous sheath, or acrosomal vesicle (Fig. 5C). Examples of components of the microtubule-based axoneme with an increased expression level are *Dnah5* (Dynein axonemal heavy chain protein 5), *Odad2* (Outer dynein arm docking complex subunit 2), *Ccdc103* (Coiled-coil domain containing 103), *Cfap69* (Cilia and flagella-associated protein 69), or *Akap14* (A kinase anchor protein 14). In total, we found 12 members of the cilia and flagella-associated proteins (CFAP), 20 members of the coiled-coil domain-containing (CCDC) family, and 3 members of the tektin family (TEKT1, TEKT2, and TEKT3), all of which encompass the network of proteins that participate in cilium or flagellum-dependent cell motility (Fig. 5D). Among these, many are testis-specific or testis-enriched and associated with sperm motility. Other relevant up-regulated genes with roles in spermatogenesis and male reproduction are eight members of the Spata family, the testis-specific kinases *Tssk3* and *Tssk4*, three Spaca genes, three lysozyme-like genes, and the subunits of the sperm-specific calcineurin *Ppp3r2* and *Ppp3cc*. Consistent with these findings, the GO-MF overrepresentation analysis revealed protein phosphatase regulator and lysozyme activities.

The GO-BP enriched in down-regulated genes are, as summarized in Fig. 5B, steroid metabolism, oxidative stress, and peptidyl-tyrosine phosphorylation. Regarding molecular functions, many of the GO-MF terms are related with oxidoreductase

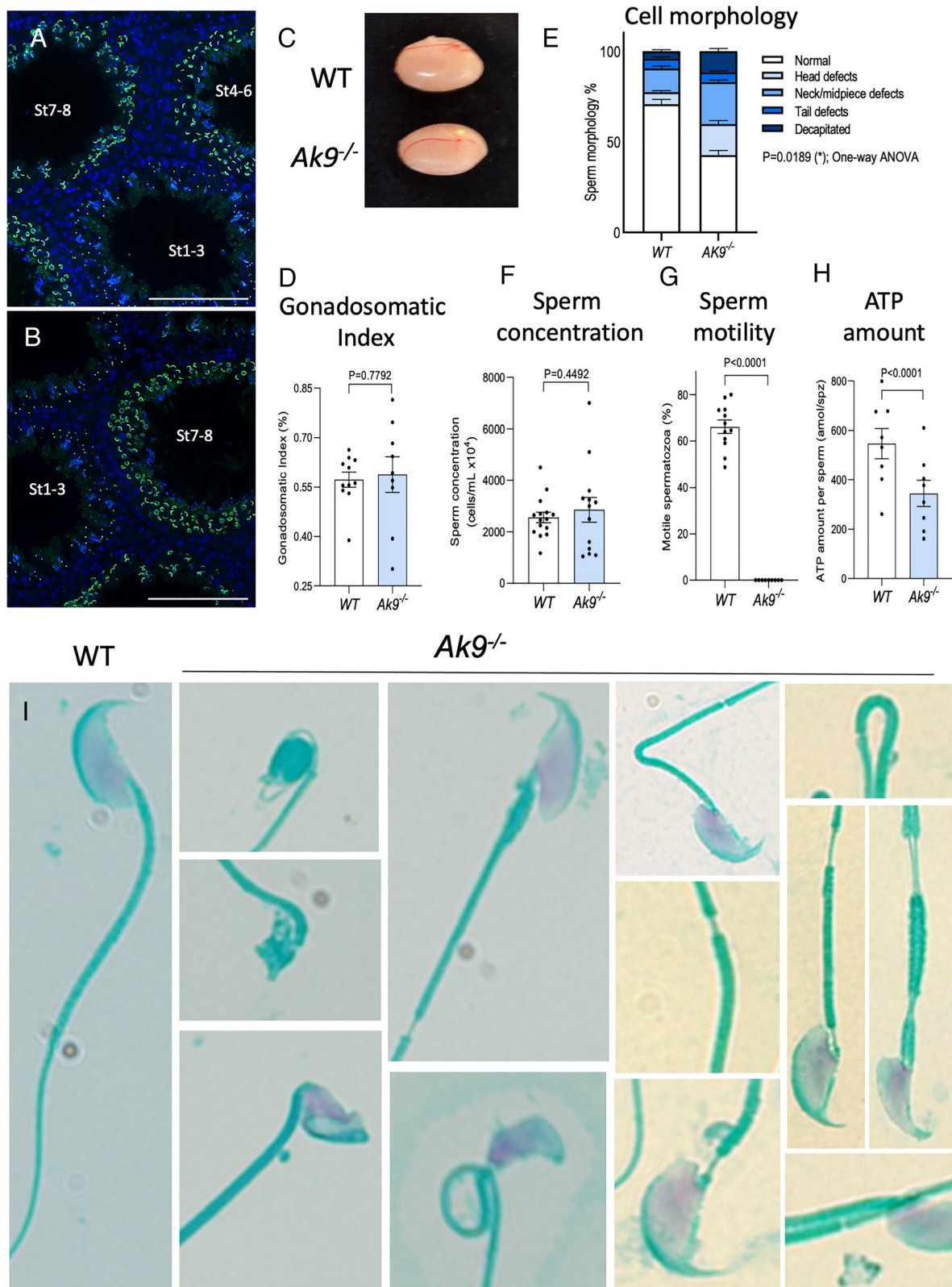


**Fig. 4.** Evaluation of sperm and testis in  $Ak9^{WT}$  and  $Ak9^{-/-}$  mice. (A) Cross-sections of seminiferous tubules stained with nuclear dye Hoechst (blue) and acrosome PNA-FITC labelling (green) in  $Ak9^{WT}$  mice and (B)  $Ak9^{-/-}$  mice. (C) Images of whole testes from WT and  $Ak9^{-/-}$  mice. (D) Gonad/body size ratio of WT ( $n = 11$ ) and  $Ak9^{-/-}$  ( $n = 9$ ) mice. Student's  $t$ -test  $P > 0.05$ . (E) Significant differences in sperm morphology categories between WT ( $n = 7$ ) and  $Ak9^{-/-}$  ( $n = 9$ ) mice. One-way ANOVA  $P < 0.05$ . (F) Sperm concentration of WT ( $n = 15$ ) and  $Ak9^{-/-}$  ( $n = 12$ ) mice. Student's  $t$ -test  $P > 0.05$ . (G) Pronounced difference in percentage of motile sperm between WT ( $n = 12$ ) and  $Ak9^{-/-}$  ( $n = 9$ ) mice (Student's  $t$ -test  $P < 0.05$ ). (H) ATP amount per sperm (amol/spz) (Student's  $t$ -test  $P < 0.05$ ). (I) Examples of morphological abnormalities of  $Ak9^{-/-}$  sperm. Data are presented as mean  $\pm$  SEM.

activity (Dataset S4). These processes and functions are associated with the energy state of the cell so that the impaired energy production or distribution may lead to sperm with no ability to move.

**Sperm from  $Ak9^{-/-}$  Mice Exhibit Ultrastructural Defects of the Flagellum.** Ultrastructure analysis of sperm cells from  $Ak9^{-/-}$  mice was performed by transmission electron microscopy and showed a



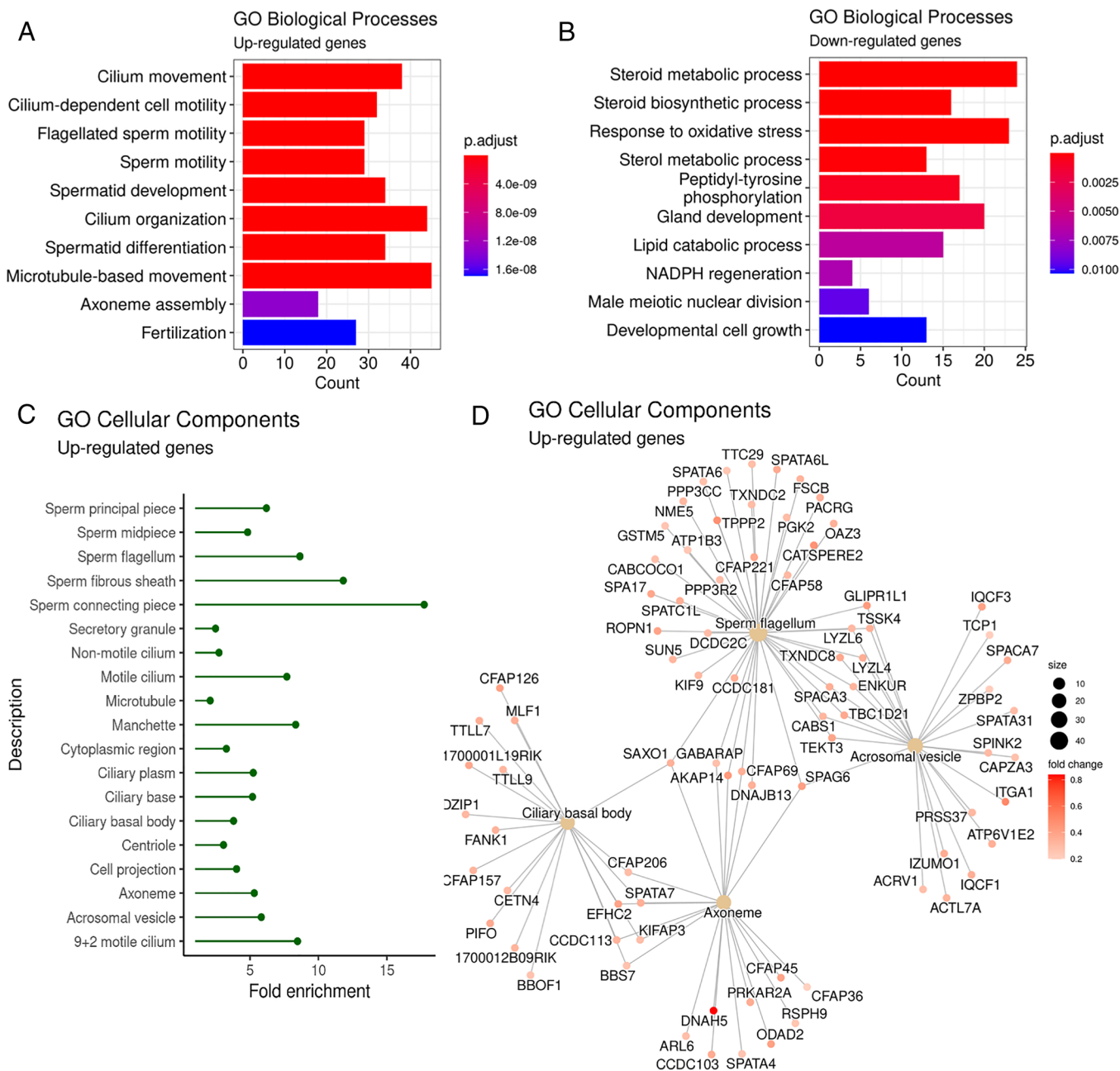


**Fig. 5.** Gene ontology annotation of differentially expressed genes in *Ak9<sup>-/-</sup>*. (A) Top 10 significant biological process GO terms with overrepresentation in up-regulated and (B) down-regulated genes showing the adjusted *P*-value and the gene count. (C) Cellular components enriched in the set of up-regulated genes, where the *x*-axis displays the fold enrichment over the annotated ratio. (D) Representative cellular components and their associated genes. Fisher's exact test FDR < 0.05.

severe disorganization of the (9 + 2) axonemal structure, in particular, disorganization of the axonemal structure with lack of the peripheral and/or central pair of microtubules (Fig. 6 A–E). Also, abnormal flagella with several axonemal pieces within the same cytoplasmic membrane were observed (Fig. 6 A–C). Both in the midpiece and principal piece, the *Ak9<sup>-/-</sup>* sperm exhibited a higher percentage of abnormal axonemal morphology (Fig. 6 I and J).

## Discussion

Here, we report the identification of an intronic variant in the bovine *AK9* gene that activates cryptic splicing, correlated with extreme subfertility in bulls. This mutation is correlated with impaired sperm hyperactivation and compromised ability to bind to and penetrate the oocyte, resulting in extremely low rates of

fertilization and embryo development. To further investigate the function of *AK9*, we generated *AK9*-deficient mice. These mice exhibited normal sperm production but substantial impairments in sperm motility, characterized by reduced ATP concentration and abnormal morphology, particularly microtubular flagellar alterations, resulting in infertility. These observations are consistent with the results obtained from testes RNA-seq analysis, confirming the impact of the gene alteration. The observed differences in sperm motility between the bull (FR4854) and *AK9*-deficient mice are likely attributed to the partial knockout nature in the bull, where a small amount of normal *AK9* transcripts persist. Additionally, differences in sperm metabolism between bulls and mice could play a role. While the lack of ATP could have a drastic effect on mouse sperm motility, it is less apparent in bulls, where it is primarily required for hyperactivation. For example, when

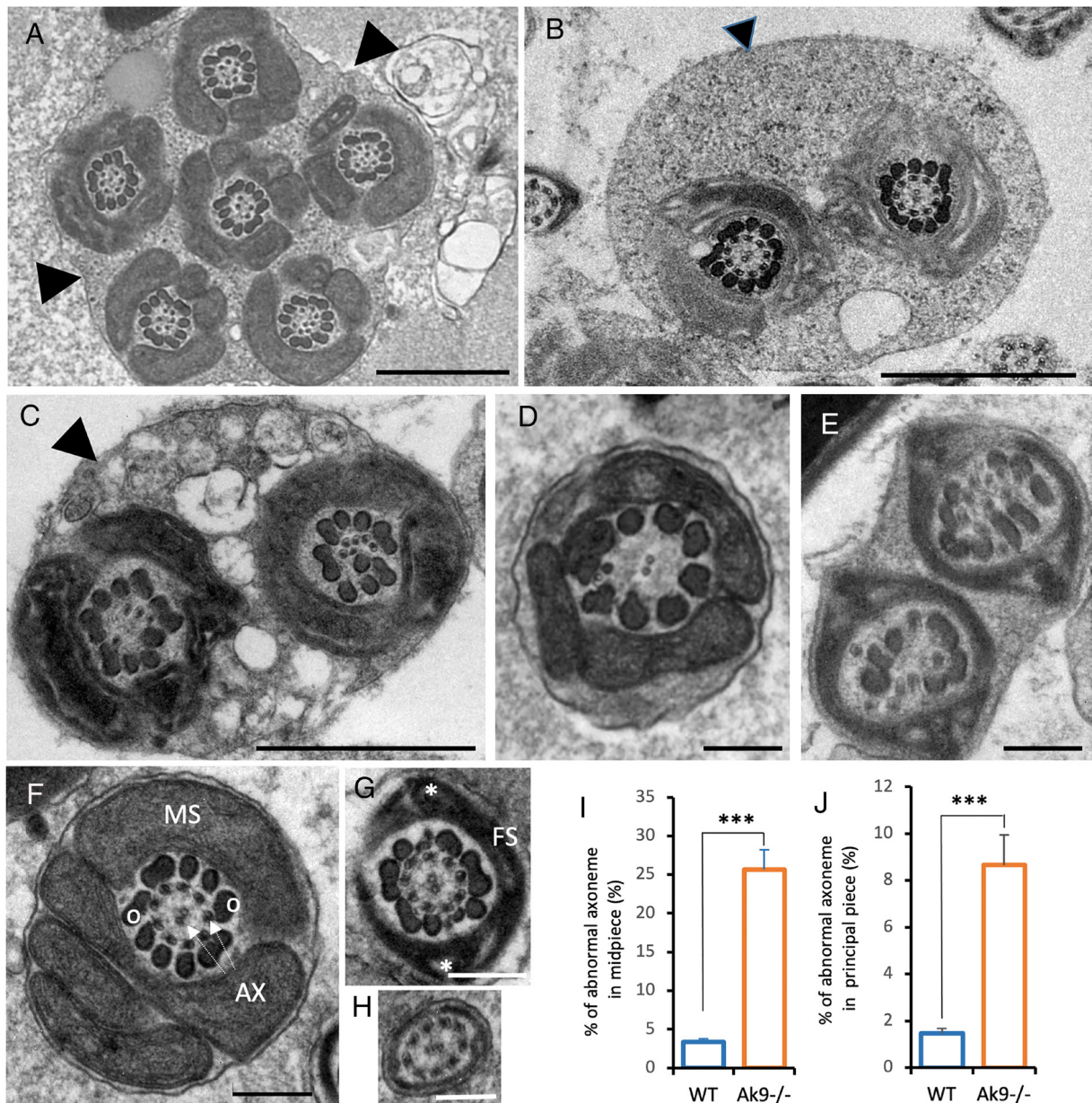


**Fig. 6.** Transmission electron microscopy (TEM) cross-sections of *Ak9*<sup>-/-</sup> and wild-type mice sperm flagella. Representative TEM cross-sections of sperm flagella at the mid-piece (A–D) and principal piece (E) of *Ak9*<sup>-/-</sup> mutant; and mid-piece (F), principal piece (G), and endpiece (H) of wild-type mice. In the wild-type, the axoneme (AX) exhibits a typical “9 + 2” microtubule structure comprising nine peripheral microtubule doublets paired associated with nine outer dense fibers (o) and the central pair of microtubules. In the mid-piece (F) a helically arranged mitochondrial sheath (MS) surrounds the axoneme. At the proximal principal piece (G) mitochondria are replaced by the Fibrous Sheath (FS), which is organized in two longitudinal columns (\*) that replace outer dense fibres 3 and 8 and are joined by transverse hemi-circumferential “ribs” (FS). (A–E) Many of the spermatozoa from *Ak9*<sup>-/-</sup> male mice present disordered peripheral and central microtubules. The images A, B, C, and E show several pieces cut transversely within the same cytoplasmic membrane (indicated with arrowheads). (I and J) Quantification ratio of abnormal axoneme in midpiece (I) and principal piece (J) of WT and *Ak9*<sup>-/-</sup> spermatozoa. Data are presented as mean ± SEM. A two-tailed Student’s *t* test was performed, \*\*\**P* < 0.001. Scale bar 1 μm (A–C) and 300 nm (D–H).

the energy source (glucose, pyruvate, and lactate) is removed from sperm media, mouse sperm stop moving immediately, while bull sperm can continue to move for several hours, indicating less dependence on the glycolytic pathway compared to mice (19). It has been reported that bovine sperm motility is facilitated by fatty acids (20). However, many studies have revealed that an active glycolytic pathway is necessary for the normal occurrence of sperm hyperactivation in mice and humans (21, 22).

A plethora of assays has been used to predict the field fertility of bulls used in AI. Many of these assays are poorly correlated with field fertility with only about 40–50% of the variation in male fertility being explained under the best circumstances (23, 24). In the current study, none of the parameters assessed by flow cytometry was

different between FR4854 and a control fertile bull. CASA indicated differences in a range of sperm motility parameters between FR4854 and a panel of bulls of known fertility. Importantly, sperm from FR4854 exhibited much reduced caffeine-induced hyperactivation which may explain the failure to penetrate oocytes following IVF or to reach the site of fertilization and bind with and penetrate the oocyte in vivo in superovulated heifers. Hyperactivation of the sperm, characterised by high-amplitude, asymmetrical flagellar bending, is critical for fertilization, as it is required for penetration of the zona pellucida (25, 26). Hyperactivation may also facilitate release of sperm from the oviductal storage reservoir and may propel sperm through mucus in the oviductal lumen and the matrix of the cumulus–oocyte complex (25).



It is interesting and somewhat counterintuitive that despite the failure to penetrate the oocyte after IVF (based on assessment of pronuclei at 17 hpi), or a much-reduced capacity to penetrate empty zonae, oocytes inseminated with semen from FR4854 exhibited some, albeit much reduced, mitotic cleavage. However, it is important to note that this cleavage was not normal, being very delayed (most arrested at the 2-cell stage) and exhibiting abnormal fragmentation/asymmetrical blastomeres. The kinetics of the early cleavage divisions has long been recognized as a marker of oocyte developmental competence (27). In cattle, the sire can affect the timing of the onset and duration of this DNA replication during the first cell cycle, and thereby ultimately influence the timing of the first cleavage division (28–30). In the present study, after IVF, FR4854 displayed little evidence of normal fertilization (based on proportion of presumptive zygotes arrested in metaphase II at 17 hpi), a low cleavage rate, and delayed kinetics of cleavage (based on the number of >5-cell embryos at 48 hpi). Consistent with previous studies (30), this delayed kinetics of cleavage resulted in a very low blastocyst yield compared to the control. Consistent with the IVF data, following insemination of superovulated heifers, FR4854 displayed very low fertilization rate, delayed cleavage kinetics, and almost no accessory sperm (1 sperm on one of 131 structures recovered).

The routine evaluation and recording of tens of thousands of ejaculates and millions of artificial inseminations occasionally detect bulls with aberrant semen quality or strikingly low fertility following inseminations (4). Impaired semen quality and low fertility in healthy bulls can be caused by deleterious alleles at genes that show testis-biased or testis-specific expression (4, 11, 12). Such alleles can be spread disproportionately by females because they are typically not impacted by defective genes that are primarily expressed in the male reproductive system. We suspect that this is also true for AK9 loss-of-function alleles since we did not detect deleterious phenotypes in homozygous females in either cattle or in mice. Semen quality and male fertility are only evaluated in breeding bulls. Thus, recessive variants that compromise male reproduction can remain undetected in cattle populations for a long period of time or reach a high allele frequency without being detected (4).

We hypothesized that the drastically reduced fertility of FR4854 was due to a recessively inherited allele that is deleterious to protein function. A step-wise approach to identify the causal mutation underlying the subfertility was undertaken involving whole-genome sequencing from semen and subsequent reference-guided variant detection, detection of segments of extended autozygosity, variant annotation to predict consequences of polymorphic sites, variant filtration against a reference dataset to identify variants unique to FR4854, and, finally, validation by whole-transcriptome sequencing of testicular tissue recovered at slaughter. This process identified an intronic variant (Chr9:40620329A>G) in *AK9* encoding adenylate kinase 9 which was immediately interesting due to the testis-biased expression of *AK9* in mammals. The mutant G allele, for which FR4854 is homozygous, introduces a novel canonical splice donor site that results in a frameshift in translation and a severely truncated protein. The vast majority of *AK9* transcripts are affected by this impaired splicing. However, a small amount (~7%) of regularly spliced *AK9* mRNA is produced in FR4854. Low abundance of *AK9* may be sufficient to enable fertilization in principle and may explain the low number of successful pregnancies small number of offspring attributable to this bull.

Abdollahi-Arpanahi et al. (31) prioritized a set of nonsense mutations, missense mutations, and frameshift variants carried by low-fertility Holstein bulls. Interestingly, they investigated, among others, a genomic region located on BTA9 at  $43.7 \pm 5$  Mb which contains *AK9*. This region had been associated previously with recessively inherited impaired bull fertility in the Holstein breed (32, 33).

While Abdollahi-Arpanahi et al. (31) prioritized the Chr9:40620329A>G variant as a candidate causal variant for impaired bull fertility, the use of a flawed Ensembl annotation assigned the wrong functional consequence to the variant precluding an in-depth investigation. We reveal association of the Chr9:40620329A G-allele with extreme subfertility in a Holstein bull based on a different methodological approach and an independent cohort of animals. Moreover, we provide compelling evidence that the Chr9:40620329A>G variant activates cryptic splice sites and so results in a shortened *AK9* transcript that may either be retained with an impaired function or be degraded via nonsense-mediated mRNA decay. Drastically reduced abundance of *AK9* in FR4854 may suggest the latter.

Adenylate kinases are enzymes that maintain nucleoside balance and play a role in various cellular processes involving metabolism and nucleotide signaling (34, 35). There are nine different forms of adenylate kinases, each with distinct expression patterns across tissues and subcellular localizations, suggesting their essential and diverse roles (36, 37). They contribute to energy distribution within cells by transferring ATP from its source to sites where it is needed, replenishing ATP in processes that require rapid consumption. Adenylate kinases are also involved in specific cellular activities such as muscle contraction, hormone secretion, nuclear transport, and cell motility (38). The adenylate kinase-catalyzed phosphotransfer system regulates cell motility by interacting with the microtubular structure of cilia and flagella, thus modulating energy distribution (39, 40). Several mechanisms related to nucleotide dynamics have been associated with sperm motility, including ATP-dependent dyneins, proteins responsible for generating force in axonemes, and cyclic AMP signaling that drives sperm capacitation and hyperactivation, characterized by increased flagellar bending amplitude and asymmetry (41). Therefore, proper energy distribution and maintenance of nucleoside balance are crucial for acquiring sperm motility and transitioning through different motility patterns. In this context, specific adenylate kinases, such as AK1, AK2, AK7, and AK8, have been identified in sperm flagellum structures, and their elimination has been shown to impair sperm motility (42–45). Additionally, in many nonmammalian species, AK family members are closely associated with the axoneme in cilia and flagella (44). Adenylate kinase 9 is the most recent adenylate kinase identified in humans and is conserved in eukaryotes. AK9 functions as a nucleoside mono- and diphosphate kinase, playing a role in nucleoside homeostasis (46). It exhibits a preference for catalyzing the phosphorylation of AMP and CDP. AK9 is involved in providing NTPs for N-glycosylation and defects in AK9 have been associated with limb girdle type congenital myasthenic syndrome (47). Of particular note, AK9 is prominently expressed in the testes of mice and humans (48, 49) as well as in sheep testes compared to other tissues (49, 50).

Adenylate kinase activity was initially implied in bull sperm flagella in experiments reported by Lindemann and Rikmenspoel (51) and confirmed by Schoff, Cheetham and Lardy (52). Adenylate kinases 1 and 2 are part of the accessory structures in the mouse sperm flagellum (42, 53). Interestingly, AK1 protein was more expressed in sperm from high fertility than low fertility Holstein bulls (54), although abundance did not differ between immotile and motile subpopulations. Nonetheless, presence in both bovine and murine sperm flagella strongly suggests a function in motility in these species. The fluctuation of nucleotide concentrations in normal and metabolically stimulated sperm suggests that AK1 is mostly active when the cell is highly motile (52). According to these authors, AK1 would ensure the availability of additional energy in times of increased demand, for example, to produce the high amplitude flagellar bends characteristic of hyperactivated motility (55). In mice,



*Ak7*<sup>-/-</sup> males exhibit spermatogenesis defects manifested by almost complete absence of mature spermatids and spermatozoa in the seminiferous tubules, absence of mature sperm in the epididymis, and consequent male infertility (56). In humans, morphological abnormalities of the sperm flagellum have been associated with a homozygous missense mutation in AK7 leading to primary male infertility and multiple morphological abnormalities of the flagellum (43, 57). Prior to the current study, no direct evidence existed for a role of AK9 in male fertility; however, consistent with the reduced ability to exhibit hyperactivation by FR4854, combined evidence suggests a relationship between adenylate kinases and male fertility through sustaining energy needs during hyperactivated sperm motility.

Our results show that 30% of murine *Ak9*<sup>-/-</sup> spermatozoa has abnormalities in the structure of the flagella and their microtubules; however, 100% of the spermatozoa have compromised motility, indicating that these structural alterations are not the cause of immobility. The mechanisms for the association of *AK9*<sup>-/-</sup> with sperm microtubular and flagellar structures are unknown. However, it has been reported that *Ak7* mutations are also associated with primary ciliary dyskinesia in mice (56). There are different processes involved that enable different AK isoforms to be compartmentalized with specific sperm structures (e.g., mitochondria, outer dense fibers, and axonemes). For example, AK8 is rich in prolines that are distributed throughout the primary structure of the protein may be involved in binding to other proteins of a complex that may buffer energy levels within microdomains of the sperm flagellum (44). Other AKs previously reported to localize to the sperm flagella, AK1 and AK2, associate with the integral protein outer dense fiber 4 (ODF4) to control energy metabolism for sperm shape (flagellar straightening) and movement (53). We found that AK9 is expressed in round spermatids in bull and mouse testis, and AK9 protein production may coincide with flagellar biogenesis. It is possible that AK9 and other AKs are essential for flagellar biogenesis, and that the presence of several AKs in the spermatid may allow for compensation of function in the absence of AK9.

Knockout *Ak9*<sup>-/-</sup> mice exhibited an altered transcript profile in many testis genes, although the vast majority of the genes show small differences, and the majority of the differences were exhibited during the spermatocyte and spermatid stages, when the principal expression of AK9 protein was observed by immunofluorescence. While there are theoretical mechanisms through which adenylate kinase could potentially affect gene expression (e.g., through modulation of transcription factors or coactivators/co-repressors involved in gene transcription or through ATP-dependent chromatin remodeling), the direct role of adenylate kinases in gene regulation is not well established and is an area of ongoing research. Gene expression is a complex process influenced by a multitude of factors, and the role of adenylate kinases in this context is likely to be indirect and intertwined with broader cellular signaling and metabolic pathways.

Although in female AK9-deficient mice, no decrease in fertility or any other affected phenotype is observed, whether or not AK9 plays any role in cattle female reproduction is unclear. Interestingly, AK9 was among unique proteins identified in plasma exosomes of low-fertility heifers (58). Also, *AK9* was differentially expressed in the endometrium on Day 7 postpartum in cows between cows which remained healthy and cows which subsequently developed purulent vaginal discharge (59). We examined the distribution of the fertility of half-sibling sisters of FR4854 and compared them to the 2021 born population for comparison (the majority of his inseminations were in 2020 so would have resulted in 2021 offspring). Interestingly, his half-siblings were behind the mean of the overall population for overall EBI, production, fertility, and calving interval PTA. Further analysis is required to confirm whether this is related in any way to AK9.

In conclusion, we have described an intronic variant that activates cryptic splicing of the adenylate kinase 9 gene correlated with extreme male subfertility in cattle and demonstrate that the phenotypic consequence of this mutation is altered sperm hyperactivation and a compromised ability to bind to and penetrate the oocyte. Mice deficient in AK9 produced immotile sperm that were incapable of normal fertilization. The widespread use of individual sires for AI potentially promotes the propagation of recessive conditions. Inadvertent matings between unknown carriers of deleterious alleles may result in the manifestation of subfertile or fatal phenotypes in their progeny. Therefore, these results could aid in the development of novel genomic tools that allow early detection and culling of subfertile bulls (60).

## Materials and Methods

Sperm morphology and function were assessed using a range of assays including light and electron microscopy, computer-assisted sperm analysis, flow cytometry, mucus penetration, in vitro and in vivo fertilization, and immunohistochemistry of testes tissue. A step-wise approach to identify the causal mutation underlying the subfertility in FR4854 was undertaken involving whole-genome sequencing from semen and subsequent reference-guided variant detection, detection of segments of extended autozygosity, variant annotation to predict consequences of polymorphic sites, variant filtration against a reference dataset, and, finally, validation by whole-transcriptome sequencing of testicular tissue recovered at slaughter. Mice deficient in AK9 were generated by CRISPR/Cas9 technology to further investigate the function of the gene. Sperm function was fully characterized and RNA-seq analysis of their testis to identify differential gene expression associated with the phenotype.

Full details of the methods are available in *SI Appendix*.

**Data, Materials, and Software Availability.** Whole-genome DNA and RNA sequencing data of FR4854 are available at the European Nucleotide Archive (ENA) of the EMBL at the BioProject [PRJEB60952](https://www.ebi.ac.uk/ena/browser/view/PRJEB60952) (61) under sample accession [SAMEA112843208](https://www.ebi.ac.uk/ena/browser/view/SAMEA112843208). Mouse testis RNA-seq data have been deposited at GEO and are publicly available. The accession number for the raw and processed data files is [GSE235546](https://www.ncbi.nlm.nih.gov/geo/query/acc.cgi?acc=GSE235546) (62).

**ACKNOWLEDGMENTS.** We are thankful for the excellent support provided by Dimitri Scholz and Tiine O'Neill from the Biological Imaging facility in University College Dublin Conway Institute for electron microscopy and the ETH Zürich technology platform Functional Genomics Center Zurich (<https://fgcz.ch/>) for DNA and RNA sequencing. We gratefully thank Centro de Supercomputación de Galicia (Supercomputing Center of Galicia) for providing the necessary resources for the data processing. Portions of the paper were developed from the thesis of E.O. This work was funded by Science Foundation Ireland to P.L., S.F. and D.A.K (Project 16/IA/4474). X.M.M., A.L.-V., and H.P. received financial support from Swissgenetics, Zollikofen, Switzerland (<https://swissgenetics.ch/>), the Swiss NSF (310030-185229), and through an ETH Research Grant. A.G.-A., P.N.-L., M. Maroto, R.F.-G., and E.P. were supported by Grant PID2021-1225070B-I00, and M.B.-A., M.A by Grant PID2021-123091NB-C21, both funded by MCIN/AEI/10.13039/501100011033/ and European Union NextGenerationEU/PRTR. J.M.S. was funded by Talent Attraction Program of the Comunidad de Madrid (AT2019-T2-BIO-12966). P.N.-L. was supported by a pre-doctoral fellowship from the Spanish Ministry of Science and Innovation (MICINN) (PRE2019-088813).

Author affiliations: <sup>a</sup>Animal and Crop Sciences, School of Agriculture and Food Science, University College Dublin, Belfield, Dublin D04 V1W8, Ireland; <sup>b</sup>Departamento de Reproducción Animal, Instituto Nacional de Investigación y Tecnología Agraria y Alimentaria-Centro Nacional integrado en la Agencia Estatal Consejo Superior de Investigaciones Científicas, Madrid 28040, Spain; <sup>c</sup>Department of Biological Sciences, Bernal Institute, Faculty of Science and Engineering, University of Limerick, Limerick V94 T9PX, Ireland; <sup>d</sup>National Cattle Breeding Centre, County Kildare W91 WF59, Ireland; <sup>e</sup>Irish Cattle Breeding Federation, Link Road, Ballincollig, County Cork P31 D452, Ireland; <sup>f</sup>Animal Genomics, Institute of Agricultural Sciences, ETH Zürich, Zürich 8092, Switzerland; <sup>g</sup>Departamento de Biología Celular e Histología, Universidad de Murcia-Instituto Murciano de Investigación Biosanitaria Pascual Parrilla, Murcia 30120, Spain; <sup>h</sup>Departamento de Biodiversidad y Biología Evolutiva, Museo Nacional de Ciencias Naturales, Madrid 28006, Spain; and <sup>i</sup>Animal and Bioscience Department, Teagasc, Animal and Grassland Research and Innovation Centre, Grange, Dunsany, County Meath C15 PW93, Ireland

1. R. P. Amann, J. M. DeJarnette, Impact of genomic selection of AI dairy sires on their likely utilization and methods to estimate fertility: A paradigm shift. *Theriogenology* **77**, 795–817 (2012).
2. L. Shalloo, A. Cromie, N. McHugh, Effect of fertility on the economics of pasture-based dairy systems. *Animal* **8**, 222–231 (2014).
3. S. Fair, P. Lonergan, Review: Understanding the causes of variation in reproductive wastage among bulls. *Animal* **12**, s53–s62 (2018).
4. H. Pausch *et al.*, A nonsense mutation in TMEM95 encoding a nondescript transmembrane protein causes idiopathic male subfertility in cattle. *PLoS Genet.* **10**, e1004044 (2014).
5. B. Fernandez-Fuertes *et al.*, Subfertility in bulls carrying a nonsense mutation in transmembrane protein 95 is due to failure to interact with the oocyte vestments. *Biol. Reprod.* **97**, 50–60 (2017).
6. I. Lamas-Toranzo *et al.*, TMEM95 is a sperm membrane protein essential for mammalian fertilization. *eLife* **9**, e53913 (2020).
7. T. Noda *et al.*, Sperm proteins SOF1, TMEM95, and SPACA6 are required for sperm-oocyte fusion in mice. *Proc. Natl. Acad. Sci. U.S.A.* **117**, 11493–11502 (2020).
8. M. C. McClure *et al.*, SNP data quality control in a National Beef and Dairy Cattle System and highly accurate SNP based parentage verification and identification. *Front. Genet.* **9**, 84 (2018).
9. M. Hiltbold *et al.*, A 1-bp deletion in bovine QRICH2 causes low sperm count and immature sperm with multiple morphological abnormalities. *Genet. Sel. Evol.* **54**, 18 (2022).
10. M. Hiltbold *et al.*, Activation of cryptic splicing in bovine WDR19 is associated with reduced semen quality and male fertility. *PLoS Genet.* **16**, e1008804 (2020).
11. T. Iso-Touru *et al.*, A splice donor variant in CCDC189 is associated with asthenospermia in Nordic Red dairy cattle. *BMC Genomics* **20**, 286 (2019).
12. H. Pausch *et al.*, A frameshift mutation in ARMC3 is associated with a tail stump sperm defect in Swedish Red (*Bos taurus*) cattle. *BMC Genet.* **17**, 49 (2016).
13. B. J. Hayes, H. D. Daetwyler, 1000 bull genomes project to map simple and complex genetic traits in cattle: Applications and outcomes. *Annu. Rev. Anim. Biosci.* **7**, 89–102 (2019).
14. M. Cescon, F. Gattazzo, P. Chen, P. Bonaldo, Collagen VI at a glance. *J. Cell Sci.* **128**, 3525–3531 (2015).
15. L. Fang *et al.*, Comprehensive analyses of 723 transcriptomes enhance genetic and biological interpretations for complex traits in cattle. *Genome Res.* **30**, 790–801 (2020).
16. A. Dobin *et al.*, STAR: Ultrafast universal RNA-seq aligner. *Bioinformatics* **29**, 15–21 (2013).
17. S. Liu *et al.*, A multi-tissue atlas of regulatory variants in cattle. *Nat. Genet.* **54**, 1438–1447 (2022).
18. C. D. Green *et al.*, A comprehensive roadmap of murine spermatogenesis defined by single-cell RNA-Seq. *Dev. Cell* **46**, 651–667.e610 (2018).
19. F. A. Navarrete *et al.*, Transient sperm starvation improves the outcome of assisted reproductive technologies. *Front. Cell Dev. Biol.* **7**, 262 (2019).
20. M. M. Islam, T. Umehara, N. Tsujita, M. Shimada, Saturated fatty acids accelerate linear motility through mitochondrial ATP production in bull sperm. *Reprod. Med. Biol.* **20**, 289–298 (2021).
21. C. I. Marin-Briggiler *et al.*, Human sperm remain motile after a temporary energy restriction but do not undergo capacitation-related events. *Front. Cell Dev. Biol.* **9**, 777086 (2021).
22. M. Tourmente, E. Sansegundo, E. Rial, E. R. S. Roldan, Capacitation promotes a shift in energy metabolism in murine sperm. *Front. Cell Dev. Biol.* **10**, 950979 (2022).
23. N. C. Bernecic *et al.*, Comprehensive functional analysis reveals that acrosome integrity and viability are key variables distinguishing artificial insemination bulls of varying fertility. *J. Dairy Sci.* **104**, 11226–11241 (2021).
24. E. Sellem *et al.*, Use of combinations of in vitro quality assessments to predict fertility of bovine semen. *Theriogenology* **84**, 1447–1454.e1445 (2015).
25. S. S. Suarez, Control of hyperactivation in sperm. *Hum. Reprod. Update* **14**, 647–657 (2008).
26. M. Zaferani, S. S. Suarez, A. Abbaspourad, Mammalian sperm hyperactivation regulates navigation via physical boundaries and promotes pseudo-chemotaxis. *Proc. Natl. Acad. Sci. U.S.A.* **118**, e2107500118 (2021).
27. P. Lonergan *et al.*, Effect of time interval from insemination to first cleavage on the developmental characteristics, sex ratio and pregnancy rate after transfer of bovine embryos. *J. Reprod. Fertil.* **117**, 159–167 (1999).
28. P. Comizzoli, B. Marquant-Le Guienne, Y. Heyman, J. P. Renard, Onset of the first S-phase is determined by a paternal effect during the G1-phase in bovine zygotes. *Biol. Reprod.* **62**, 1677–1684 (2000).
29. L. N. Eid, S. P. Lorton, J. J. Parrish, Paternal influence on S-phase in the first cell cycle of the bovine embryo. *Biol. Reprod.* **51**, 1232–1237 (1994).
30. F. Ward *et al.*, Paternal influence on the time of first embryonic cleavage post insemination and the implications for subsequent bovine embryo development in vitro and fertility in vivo. *Mol. Reprod. Dev.* **60**, 47–55 (2001).
31. R. Abdollahi-Arpanahi, H. A. Pacheco, F. Penagaricano, Targeted sequencing reveals candidate causal variants for dairy bull subfertility. *Anim. Genet.* **52**, 509–513 (2021).
32. J. P. Nani, F. M. Rezende, F. Penagaricano, Predicting male fertility in dairy cattle using markers with large effect and functional annotation data. *BMC Genomics* **20**, 258 (2019).
33. P. Nicolini, R. Amorin, Y. Han, F. Penagaricano, Whole-genome scan reveals significant non-additive effects for sire conception rate in Holstein cattle. *BMC Genet.* **19**, 14 (2018).
34. D. E. Atkinson, The energy charge of the adenylate pool as a regulatory parameter. Interaction with feedback modifiers. *Biochemistry-US* **7**, 4030–4034 (1968).
35. P. P. Dzeja, R. J. Zeleznikar, N. D. Goldberg, Adenylate kinase: Kinetic behavior in intact cells indicates it is integral to multiple cellular processes. *Mol. Cell Biochem.* **184**, 169–182 (1998).
36. T. Noma, Dynamics of nucleotide metabolism as a supporter of life phenomena. *J. Med. Invest.* **52**, 127–136 (2005).
37. C. Panayiotou, N. Solaroli, A. Karlsson, The many isoforms of human adenylate kinases. *Int. J. Biochem. Cell Biol.* **49**, 75–83 (2014).
38. P. Dzeja, A. Terzi, Adenylate kinase and AMP signaling networks: Metabolic monitoring, signal communication and body energy sensing. *Int. J. Mol. Sci.* **10**, 1729–1772 (2009).
39. R. van Horsen *et al.*, Modulation of cell motility by spatial repositioning of enzymatic ATP/ADP exchange capacity. *J. Biol. Chem.* **284**, 1620–1627 (2009).
40. M. Wirschell *et al.*, Oda5p, a novel axonemal protein required for assembly of the outer dynein arm and an associated adenylate kinase. *Mol. Biol. Cell* **15**, 2729–2741 (2004).
41. R. Pereira, R. Sa, A. Barros, M. Sousa, Major regulatory mechanisms involved in sperm motility. *Asian J. Androl.* **19**, 5–14 (2017).
42. W. Cao, L. Haig-Ladewig, G. L. Gerton, S. B. Moss, Adenylate kinases 1 and 2 are part of the accessory structures in the mouse sperm flagellum. *Biol. Reprod.* **75**, 492–500 (2006).
43. P. Lores *et al.*, Homozygous missense mutation L673P in adenylate kinase 7 (AK7) leads to primary male infertility and multiple morphological anomalies of the flagella but not to primary ciliary dyskinesia. *Hum. Mol. Genet.* **27**, 1196–1211 (2018).
44. M. L. Vadrnais *et al.*, Adenine nucleotide metabolism and a role for AMP in modulating flagellar waveforms in mouse sperm. *Biol. Reprod.* **90**, 128 (2014).
45. M. Xie *et al.*, Adenylate kinase 1 deficiency disrupts mouse sperm motility under conditions of energy stress. *Biol. Reprod.* **103**, 1121–1131 (2020).
46. M. Amiri, F. Conserva, C. Panayiotou, A. Karlsson, N. Solaroli, The human adenylate kinase 9 is a nucleoside mono- and diphosphate kinase. *Int. J. Biochem. Cell Biol.* **45**, 925–931 (2013).
47. C. W. Lam, K. S. Wong, H. W. Leung, C. Y. Law, Limb girdle myasthenia with digenic RAPSIN and a novel disease gene AK9 mutations. *Eur. J. Hum. Genet.* **25**, 192–199 (2017).
48. L. Fagerberg *et al.*, Analysis of the human tissue-specific expression by genome-wide integration of transcriptomics and antibody-based proteomics. *Mol. Cell Proteomics* **13**, 397–406 (2014).
49. F. Yue *et al.*, A comparative encyclopedia of DNA elements in the mouse genome. *Nature* **515**, 355–364 (2014).
50. Y. Jiang *et al.*, The sheep genome illuminates biology of the rumen and lipid metabolism. *Science* **344**, 1168–1173 (2014).
51. C. B. Lindemann, R. Rikmenspoel, Sperm flagellar motion maintained by ADP. *Exp. Cell Res.* **73**, 255–259 (1972).
52. P. K. Schoff, J. Cheatham, H. A. Lardy, Adenylate kinase activity in ejaculated bovine sperm flagella. *J. Biol. Chem.* **264**, 6086–6091 (1989).
53. C. Ito, T. Makino, T. Mutoh, M. Kikkawa, K. Toshimori, The association of ODF4 with AK1 and AK2 in mice is essential for fertility through its contribution to flagellar shape. *Sci. Rep.* **13**, 2969 (2023).
54. O. D'Amours, G. Frenette, M. Fortier, P. Leclerc, R. Sullivan, Proteomic comparison of detergent-extracted sperm proteins from bulls with different fertility indexes. *Reproduction* **139**, 545–556 (2010).
55. H. C. Ho, K. A. Granish, S. S. Suarez, Hyperactivated motility of bull sperm is triggered at the axoneme by Ca<sup>2+</sup> and not cAMP. *Dev. Biol.* **250**, 208–217 (2002).
56. A. Fernandez-Gonzalez, S. Kourembanas, T. A. Wyatt, S. A. Mitsialis, Mutation of murine adenylate kinase 7 underlies a primary ciliary dyskinesia phenotype. *Am. J. Respir. Cell Mol. Biol.* **40**, 305–313 (2009).
57. M. Xiang *et al.*, A novel homozygous missense mutation in AK7 causes multiple morphological anomalies of the flagella and oligoasthenoatozoospermia. *J. Assist. Reprod. Genet.* **39**, 261–266 (2022).
58. Y. Q. Koh *et al.*, Proteome profiling of exosomes derived from plasma of heifers with divergent genetic merit for fertility. *J. Dairy Sci.* **101**, 6462–6473 (2018).
59. A. Brewer *et al.*, Qualitative and quantitative differences in endometrial inflammatory gene expression precede the development of bovine uterine disease. *Sci. Rep.* **10**, 18275 (2020).
60. M. C. Mullen *et al.*, Development of a custom SNP chip for dairy and beef cattle breeding, parentage and research. *Interbull Bulletin* vol. 47, Nantes, France, August 23–25, 2013 (2013).
61. E. O'Callaghan *et al.*, Identification of the causal mutation underlying a case of male infertility in a Holstein bull through genome-wide DNA and RNA sequencing. European Nucleotide Archive. <https://www.ebi.ac.uk/ena/browser/view/PRJEB60952>. Deposited 30 March 2023.
62. E. O'Callaghan *et al.*, Mutations in AK9 impair male fertility by altering sperm motility in mice and cattle. *Gene Expression Omnibus*. <https://www.ncbi.nlm.nih.gov/geo/query/acc.cgi?acc=GSE235546>. Deposited 22 June 2023.